VOLUME ONE

Computed Tomography of the Whole Body

EDITED BY

JOHN R. HAAGA, M.D

Professor, Department of Radiology
Case Western Reserve University School of Medicine
of Computed Body Tomography and Division of Diag
University Hospitals of Cleveland
Cleveland, Ohio

RALPH J. ALFIDI, M.D.

VOLUME ONE

Computed Tomography of the Whole Body

EDITED BY

JOHN R. HAAGA, M.D.

Professor, Department of Radiology
Case Western Reserve University School of Medicine
Head, Section of Computed Body Tomography and Division of Diagnostic Radiology
University Hospitals of Cleveland
Cleveland, Ohio

RALPH J. ALFIDI, M.D.

Professor and Chairman, Department of Radiology
Case Western Reserve University School of Medicine
Director, Department of Radiology
University Hospitals of Cleveland
Cleveland, Ohio

Photographic Consultant, Joseph P. Molter

with 2470 illustrations

The C. V. Mosby Company

ST. LOUIS TORONTO 1983

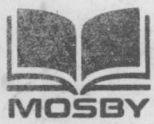

A TRADITION OF PUBLISHING EXCELLENCE

Editor: **Samuel E. Harshberger**
Assistant editor: **Anne Gunter**
Design: **Kay Kramer**
Production: **Teresa Breckwoldt, Jeanne A. Gulledge**

Two volumes

Printed in the United States of America

The C.V. Mosby Company
11830 Westline Industrial Drive, St. Louis, Missouri 63146

Library of Congress Cataloging in Publication Data

Main entry under title:

Computed tomography of the whole body.

Includes bibliographies and index.
1. Tomography. I. Haaga, John R., 1945-
II. Alfidi, Ralph J.
RC78.7.T6C6425 1983 616.07'572 82-22868
ISBN 0-8016-2047-3

C/CB/VH 9 8 7 6 5 4 3 02/C/236

Contributors

RALPH J. ALFIDI, M.D.

Professor and Chairman, Department of Radiology, Case Western Reserve University School of Medicine; Director, Department of Radiology, University Hospitals of Cleveland, Cleveland, Ohio

ALBERT AMENT, M.D.

Assistant Professor, Department of Radiology, Case Western Reserve University School of Medicine, Cleveland, Ohio

VIREN J. BALSARA, M.D.

Assistant Professor of Radiology, University of Texas Health Science Center, Houston, Texas

A. JAN BERLIN, M.D.

Head, Section of Ophthalmic Plastic and Orbital Surgery, Department of Ophthalmology, Cleveland Clinic Foundation, Cleveland, Ohio

LOUISE A. BERLIN, R.D.M.S.

Ophthalmic Sonographer, Department of Ophthalmology, Cleveland Clinic Foundation, Cleveland, Ohio

MICHAEL E. BERNARDINO, M.D.

Professor, Department of Radiology, Emory University School of Medicine, Atlanta, Georgia

CHARLES T. BONSTELLE, M.D.

Assistant Professor, Department of Radiology, Case Western Reserve University School of Medicine, Cleveland, Ohio

RICHARD S. BREIMAN, M.D.

Formerly Assistant Professor, Department of Radiology, Duke University School of Medicine, Durham, North Carolina; Currently Director of CT and Ultrasound, Samuel Merritt Hospital, Oakland, California

PATRICK J. BRYAN, M.B., F.R.C.R.

Associate Professor, Department of Radiology, Case Western Reserve University School of Medicine; Chief, Division of Ultrasound, University Hospitals of Cleveland, Cleveland, Ohio

HAROLD BUTLER, M.D.

Assistant Professor of Radiology, Case Western Reserve University School of Medicine, Cleveland, Ohio

BARBARA L. CARTER, M.D.

Professor of Radiology, Tufts University School of Medicine; Chief, CT Body Scanning and E.N.T. Radiology, New England Medical Center Hospital, Boston, Massachusetts

ROBERT J. CHURCHILL, M.D.

Associate Professor of Radiology, Loyola University of Chicago and Stritch School of Medicine, Maywood, Illinois

ALAN M. COHEN

Assistant Professor, Department of Radiology, Case Western Reserve University School of Medicine; Head, Section of Angiography, University Hospitals of Cleveland, Cleveland, Ohio

WILLIAM N. COHEN, M.D.

Clinical Professor of Radiology, State University of New York Upstate Medical Center; Attending Radiologist, Crouse-Irving Memorial Hospital, Syracuse, New York

SABA J. EL YOUSEF, M.D.

Assistant Professor, Department of Radiology, Case Western Reserve University School of Medicine, Cleveland, Ohio

CHARLES R. FITZ, M.D.

Associate Professor, University of Toronto School of Medicine; Head, Division of Special Procedures, Department of Radiology, Hospital for Sick Children, Toronto, Ontario, Canada

BARRY D. FLETCHER, M.D.

Professor, Department of Radiology, Case Western Reserve University School of Medicine; Director, Division of Pediatric Radiology, University Hospitals of Cleveland, Cleveland, Ohio

MOKHTAR GADO, M.D.

Professor of Radiology and Chief, Neuroradiology Section, Washington University School of Medicine, St. Louis, Missouri

JOHN R. HAAGA, M.D.

Professor, Department of Radiology, Case Western Reserve University School of Medicine; Head, Section of Computed Body Tomography and Division of Diagnostic Radiology, University Hospitals of Cleveland, Cleveland, Ohio

JOSEPH F. HAHN, M.D.

Chairman, Department of Neurological Surgery, Cleveland Clinic Foundation, Cleveland, Ohio

STANLEY F. HANDEL, M.D.

Clinical Professor of Radiology, Department of Diagnostic Radiology, University of Texas Medical School at Houston and M.D. Anderson Hospital and Tumor Institute, Houston, Texas

GEORGE S. HARELL, M.D.

Associate Professor of Radiology and Chief, Section of Gastrointestinal Radiology, Stanford University School of Medicine, Stanford, California

ROBERT R. HATTERY, M.D.

Professor, Mayo Medical School; Chairman, Department of Diagnostic Radiology, Mayo Clinic, Rochester, Minnesota

M. PETER HEILBRUN, M.D.

Associate Professor, Department of Neurosurgery, University of Utah College of Medicine, Salt Lake City, Utah

BARBARA C. HILL, B.A.

Technicare Corp., Solon, Ohio

WALDO S. HINSHAW, Ph.D.

Technicare Corp., Solon, Ohio

BENJAMIN KAUFMAN, M.D.

Professor, Department of Radiology, Case Western Reserve University School of Medicine; Head, Section of Neuroradiology, University Hospitals of Cleveland, Cleveland, Ohio

STEPHEN A. KIEFFER, M.D.

Professor and Chairman, Department of Radiology, State University of New York Upstate Medical Center, Syracuse, New York

MELVYN KOROBKIN, M.D.

Professor of Radiology and Chief, Computed Body Tomography, Department of Radiology, Duke University School of Medicine, Durham, North Carolina

DAVID M. KRAMER, Ph.D.

Technicare Corp., Solon, Ohio

SEUNGHO HOWARD LEE, M.D.

Professor, Department of Radiology, State University of New York Upstate Medical Center, Syracuse, New York

WALTER J. LEVY, Jr., M.D.

Assistant Professor, Department of Neurosurgery, University of Missouri School of Medicine, Columbia, Missouri

JOSEPH P. LiPUMA, M.D.

Assistant Professor, Department of Radiology, Case Western Reserve University School of Medicine; Section Head, Genitourinary Radiology, University Hospitals of Cleveland, Cleveland, Ohio

ANTHONY A. MANCUSO, M.D.

Associate Professor, Department of Diagnostic Radiology, University of Utah Medical Center, Salt Lake City, Utah

FLORO MIRALDI, Sc.D., M.D.

Professor of Engineering, Department of Biomedical Engineering, and Associate Professor, Department of Radiology, Case Western Reserve University School of Medicine; Codirector of Nuclear Radiology, University Hospitals of Cleveland, Cleveland, Ohio

MICHAEL T. MODIC, M.D.

Assistant Clinical Professor of Radiology, Case Western Reserve University School of Medicine; Neuroradiologist, Section of Neuroradiology, Cleveland Clinic Foundation, Cleveland, Ohio

SUMANT PATEL, M.D.

Assistant Professor, Department of Diagnostic Radiology, University of Texas Medical School, Houston, Texas

M. JUDITH DONOVAN POST, M.D.

Associate Professor of Radiology and Neurological Surgery, Department of Radiology, University of Miami School of Medicine, Miami, Florida

ROBERT A. RATCHESON, M.D.

Harvey Huntington Brown, Jr., Professor and Chief, Division of Neurological Surgery, Case Western Reserve University School of Medicine, Cleveland, Ohio

EDWARD N. RAUSCHKOLB, M.D.

Associate Professor, Department of Diagnostic Radiology, University of Texas Medical School, Houston, Texas

CARL M. SANDLER, M.D.

Associate Professor, Department of Radiology, University of Texas Health Science Center; Chief, Section of Uroradiology, Hermann Hospital, Houston, Texas

FRANK E. SEIDELMANN, D.O.

Clinical Associate Professor, Department of Radiology, Case Western Reserve University School of Medicine, Cleveland; Staff Radiologist, Radiology Consulting Associates, Inc., Marymount Hospital, Garfield Heights, Ohio

PHILIP R. SHALEN, M.D.

Neuroradiologist, Department of Diagnostic Radiology, Medical City Dallas Hospital, Dallas, Texas

PATRICK F. SHEEDY II, M.D.

Consultant in Diagnostic Radiology, Department of Radiology, Mayo Clinic, Rochester, Minnesota

SHELDON G. SHEPS, M.D.

Professor of Medicine, Divisions of Cardiovascular Disease and Hypertension, Mayo Medical School, Rochester, Minnesota

PAUL M. SILVERMAN, M.D.

Assistant Professor, Department of Diagnostic Radiology, Duke University Medical Center, Durham, North Carolina

ERIC H. SOLOMON, M.D.

Assistant Professor, Department of Radiology; Formerly of The University of Texas Health Science Center, Houston, Texas

ROBERT M. STEINBERG, M.D.

Instructor of Clinical Radiology, University of Texas Health Science Center; Hermann Hospital, Houston, Texas

DAVID H. STEPHENS, M.D.

Professor of Radiology, Mayo Medical School, Department of Diagnostic Radiology, Mayo Clinic, Rochester, Minnesota

SAUL TAYLOR, M.D.

Assistant Professor of Radiology, University of Minnesota Medical School; Staff Radiologist, St. Paul–Ramsey Medical Center, St. Paul, Minnesota

JONATHAN A. van HEERDEN, M.D.

Associate Professor, Department of Surgery, Mayo Clinic, Rochester, Minnesota

MEREDITH A. WEINSTEIN, M.D.

Head, Section of Neuroradiological Imaging, Department of Radiology, Cleveland Clinic Foundation, Cleveland, Ohio

HONG N. YEUNG, Ph.D.

Technicare Corp., Solon, Ohio

JESUS ZORNOZA, M.D.

Professor, Department of Diagnostic Radiology, University of Texas and M.D. Anderson Hospital and Tumor Institute, Houston, Texas

Preface

Since the introduction of computed tomography (CT) in 1974, there has been a remarkable revolution in the medical treatment of patients. The clinical use of CT has had a broad positive impact on patient management. Literally thousands of patients have been saved or their quality of life improved as a result of the expeditious and accurate diagnosis provided by CT. This improvement in diagnosis and management has occurred in all medical subspecialties, including neurological, pulmonary, cardiac, gastrointestinal, genitourinary, and neuromuscular medicine. Aside from the imaging advantages provided, the role of CT in planning and performing interventional procedures is now recognized. It is the most accurate method for guiding procedures to obtain cytological, histological, or bacteriological specimens and for performing a variety of therapeutic procedures.

The evolution and refinement of CT equipment have been as remarkable as the development of patient diagnosis. When we wrote our first book on CT, the scanning unit used was a 2-minute translate-rotate system. At the time of our second book the 18-second translate-rotate scanning unit was in general use. Currently standard units in radiological practice are third and fourth generation scanners with scan times of less than 5 seconds. All modern systems are more reliable than the earlier generations of equipment. The contrast and spatial resolution of these systems are in the range of 0.5% and less than 1 mm, respectively. The sophistication of the computer programs that aid in the diagnosis is also remarkable. There are now programs for three-dimensional reconstructions, quantitation of blood flow, determination of organ volume, longitudinal scans (Scoutview, Deltaview, Synerview, and Topogram), and even triangulation programs for performing percutaneous biopsy procedures.

CT units are now being installed in virtually every hospital of more than 200 beds throughout the United States. Most radiologists using these units are generalists who scan all portions of the anatomy. Because of the dissemination of this equipment and its use in general diagnosis, there exists a significant need for a general and complete textbook to cover all aspects of CT scanning. Our book is intended to partially supplement the knowledge of this group of physicians. We have attempted to completely and succinctly cover all portions of CT scanning to provide a complete general reference text. In planning the book, we chose to include the contributions of a large number of talented academicians with expertise different from and more complete than our own in their selected areas. By including contributors from outside our own department, we have been able to produce an in-depth textbook that combines the academic strengths of numerous individuals and departments.

The book is divided into chapters according to the organ systems, except for some special chapters on abscesses and interventional procedures. In each of the chapters the authors have organized the material into broad categories, such as congenital, benign, or neoplastic disease. Each author has tried to cover the major disease processes in each of the general categories in which CT diagnosis is applicable. Specific technical details, including the method of scanning, contrast material, collimation, and slice thickness are covered in each chapter. The interventional chapter extensively covers the various biopsy and therapeutic procedures in all the organ systems. Finally, the last chapter presents an up-to-the-minute coverage of current and recent developments in the CT literature and also provides extensive information about nuclear magnetic resonance (NMR) imaging. At this time we have had moderate experience with the NMR superconducting magnetic device produced by the Technicare Corporation and have formulated some initial opinions as to its role relative to CT and other imaging modalities. A concise discussion of the physics of NMR and a current clinical status report of the new modality are provided.

We would like to thank all those people who have worked so diligently and faithfully for the preparation of this book. First, we are very grateful to our many contributors. For photography work, we are deeply indebted to Mr. Joseph P. Molter. For secretarial and organizational skills, we are indebted especially to Mrs. Mary Ann Reid and Mrs. Rayna Lipscomb. The editorial skills of Ms. B. Hami were invaluable in preparing the manuscript. Our extremely competent technical staff included Mr. Joseph Agee, Ms. Ginger Haddad, Mrs. E. Martinelle, Mr. Mark Clampett, Mrs. Mary Kralik, and numerous others.

Finally, we are, of course, very appreciative of the support, patience, and encouragement of our wonderful families. In the Haaga family this includes Ellen, Elizabeth, Matthew, and Timothy, who provided the positive motivation and support for this book. Warm gratitude for unswerving support is also due to Rose, Sue, Lisa, Chris, Katie, Mary, and John Alfidi.

JOHN R. HAAGA
RALPH J. ALFIDI

Contents

Volume One

Volume Two

I
Imaging Principles in Computed Tomography

FLORO MIRALDI

A computed tomographic (CT) image is a display of the anatomy of a thin slice of the body developed from multiple x-ray absorption measurements made around the body's periphery. Unlike conventional tomography, where the image of a thin section is created by blurring out the information from unwanted regions, the CT image is constructed mathematically using data arising only from the section of interest. Generating such an image is confined to cross sections of the anatomy that are oriented essentially perpendicular to the axial dimension of the body (Fig. 1-1). Reconstruction of the final image can be accomplished in any plane but conventionally is performed in the transaxial plane.

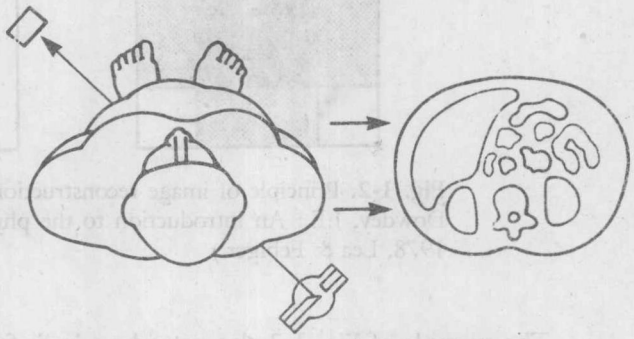

Fig. 1-1. A CT image represents the anatomy of a transaxial slice of the body obtained from many transaxial x-ray attenuation measurements.

In this chapter the physics of CT image production is discussed in qualitative terms to familiarize the practicing radiologist with the basic principles without an overwhelming amount of mathematical details. CT equipment is described, and the influence on image quality of different machine designs is discussed.

GENERAL CONSIDERATIONS

The fundamental concept in CT is that the internal structure of an object can be reconstructed from multiple projections of the object (Fig. 1-2). The object in Fig. 1-2, *A*, is composed of a number of equal blocks from which the central four have been removed to represent an internal structure. For the sake of simplicity, assume that an x-ray beam is passed through each row and column of blocks, and the transmitted radiation is measured. Since each block is the same, the measured attenuation is proportional to the number of blocks encountered in each row or column. The numbers shown at the right and beneath the object represent the relative measured attenuations, that is, the number of blocks in each row or column. These attenuation measurements are then added, as demonstrated in Fig. 1-2, *B*, to produce a numerical representation of the object (Fig. 1-2, *C*). Although this array of numbers contains all the information of the process, it is difficult to interpret and so is converted into picture form by assigning a gray scale to the numbers. Large numbers are represented by light shades of gray, and small numbers are represented by dark shades of gray. This results in the image shown in Fig. 1-2, *D*. The resultant image then can be manipulated to highlight certain areas. For example, if the gray scale is narrowed to include only black and white, then a perfect reproduction of the object is obtained by assigning black to all numbers equal to four or less and white to all numbers greater than four. In Fig. 1-2, *F*, an imperfect representation is obtained because the gray scale is chosen so that values of six and lower are black and values above six are white. In CT the method of obtaining the array of numbers is more complex, and the number of projections obtained is much greater, but the principle is the same.

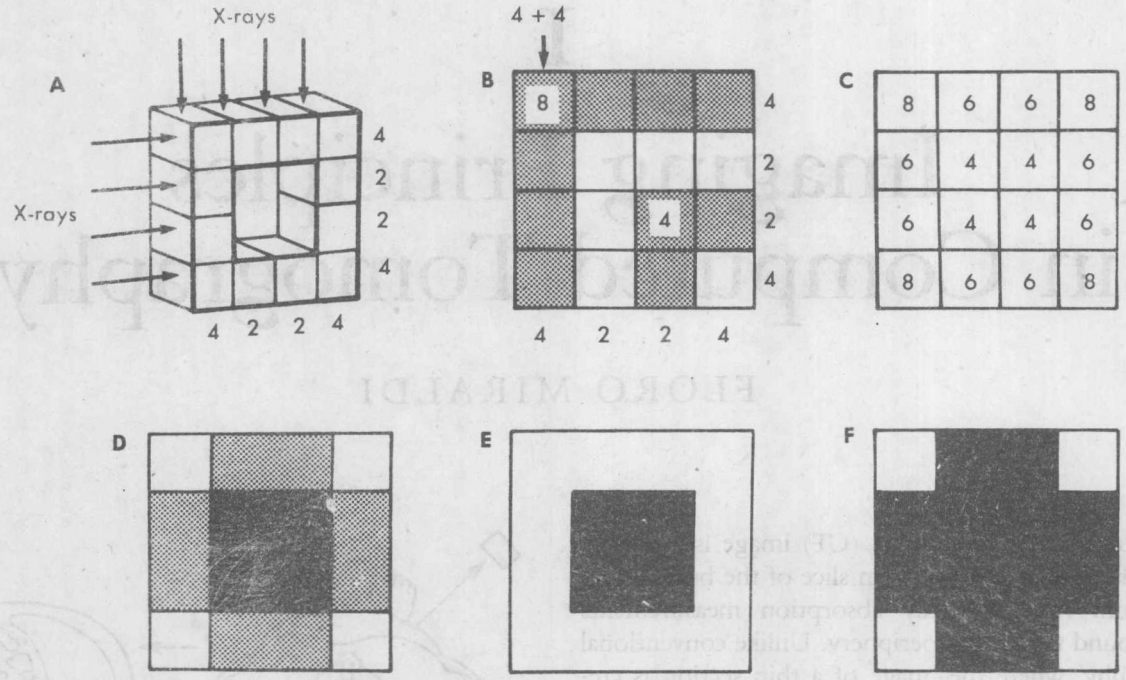

Fig. 1-2. Principle of image reconstruction. (From Christensen, E.E., Curry, T.S., III, and Dowdey, J.E.: An introduction to the physics of diagnostic radiology, ed. 2, Philadelphia, 1978, Lea & Febiger.)

The example of Fig. 1-2 also provides a basis for a number of definitions of CT terms. Each of the blocks in Fig. 1-2, *A,* represents a small attenuating volume of material and is referred to as a *voxel.* The numbers at the side and bottom of Fig. 1-2, *A,* represent single attenuation measurements and are called *ray projections,* or *ray sums.* The array of numbers in Fig. 1-2, *C,* is a *matrix,* and the individual numbers are *elements* of that matrix. Each of the blocks of gray that are used for the construction of the images in Fig. 1-2, *D* to *F,* is a *pixel.* The process of choosing the number of gray shades for a display is referred to as *selecting a window.* The *width of the window* in Fig. 1-2, *E* and *F,* is narrow, since it only contains two shades of gray (black and white) compared with the wider window of *D,* which contains three shades of gray. The number at which the window setting is centered is called the *window level.* In Fig. 1-2, *E,* the level is set at four, and in *F* it is set at six.

At first glance it appears that the procedure just outlined is awkward compared with that of conventional radiography, and it is not unreasonable to inquire why such a method is of interest. It is instructive therefore to compare radiography and CT scanning by examining the result of each modality. Both techniques are based on the x-ray attenuation equation[7,19]

$$I = I_0 e^{-\mu L} \qquad (1)$$

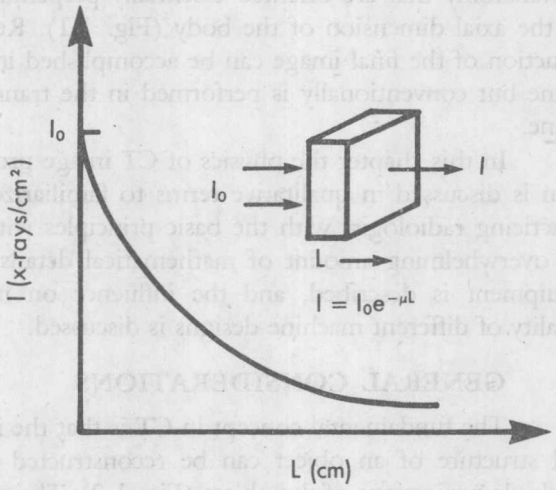

Fig. 1-3. Exponential behavior of x-ray beam attenuation.

where I_0 is the incident intensity of an x-ray beam on the surface of an object of thickness L, and I is the transmitted intensity (Fig. 1-3). The linear attenuation coefficient (μ) is a property that is dependent on the atomic number and density of the material and on the energy spectrum of the x-ray beam.[19] To present attenuation data (either I or μ) at every point throughout

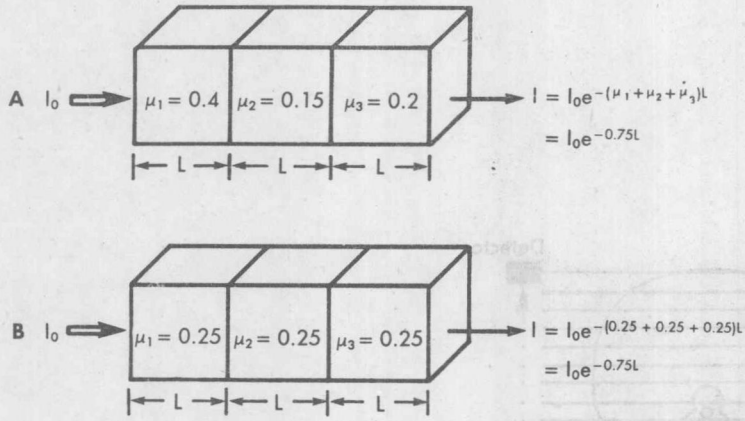

Fig. 1-4. Total attenuation of equal amount in two different cases. **A,** Nonuniform attenuation coefficients. **B,** Uniform medium.

the body would be ideal in an x-ray examination. The degree to which this is attained depends on the manner in which the measured intensities, I and I_0, are registered or manipulated. In conventional radiography the transmitted intensity (I) is seen as the darkening of a film. Because x-ray exposure of the film blackens it, the image of a dense object is lighter on the film than the image of a less dense material. In a typical radiographic film of the chest, for example, the image is light where many x-rays are absorbed or scattered, such as in bone (large μ), and dark where many x-rays are transmitted because of low absorption (small μ), such as in the regions of the lung parenchyma. Two different areas of such a chest film may show the same darkening and therefore demonstrate equal total attenuation of the beam in the two positions. However, the attenuation profile through the body may be quite different. This is diagrammatically shown in Fig. 1-4, where one beam is shown to pass through a region of relatively uniform density, where as the other beam is shown passing through a region of nonuniform densities. In conventional radiography therefore the different shades of gray seen on the film represent the differences in the transmission of an x-ray beam as it passes through the body. CT, on the other hand, approaches the ideal by presenting the average attenuation of each small volume element that comprises the body slice. Thus it unscrambles the attenuation information of the x-ray beam and presents it quantitatively with an accuracy far greater than can be accomplished by conventional techniques. This is equivalent to providing the individual values μ_1, μ_2, and μ_3 of Fig. 1-4 rather than the total value described for conventional radiography.

DATA ACQUISITION

Methods of obtaining the necessary ray projections for a CT scan require an x-ray source, detectors, and associated electronics all mounted on a *gantry,* or frame, that mechanically moves to produce the scan. Such instruments have been designed along three general lines since their introduction by Godfrey Hounsfield[17] in 1972: (1) scanners in which the x-ray tube and detectors are made to move in a translate-rotate type of mechanical motion (Fig. 1-5), (2) scanners that employ a rotating motion in which the detectors and x-ray beam rotate around the object (Fig. 1-6), and (3) scanners in which the detectors are stationary and the x-ray source is moved around the object (Fig. 1-7). A fourth type of scanner, which is not yet commercially available, utilizes multiple x-ray tubes and detectors surrounding the object, with no mechanical motion. The translate-rotate mechanical motion was the type originally developed by Hounsfield, and instruments using this original design are referred to as first generation scanners. In this machine the x-ray beam is collimated to dimensions of roughly 2 × 13 mm. The 13 mm dimension is parallel to the body axis, that is, it corresponds to the slice thickness (voxel length). The intensity of the beam is monitored by small detectors before entering the body to yield the value of the incident intensity (I_0). After passing through the body, the beam is detected by a scintillation crystal, which is also collimated to receive primarily those photons which are not scattered or absorbed. The amount of transmitted intensity (I) is then recorded and stored in the computer memory. The x-ray tube and detector system are moved continuously across the patient, making 160 multiple

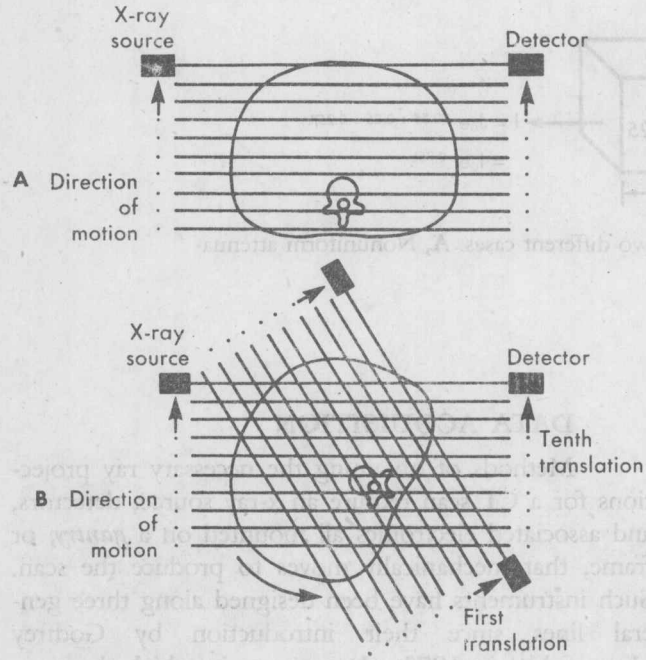

Fig. 1-5. Translate-rotate scanner. **A,** Original single detector system; single translation. **B,** Two separate translations. **C,** Second generation system with fan beam source and multiple detectors.

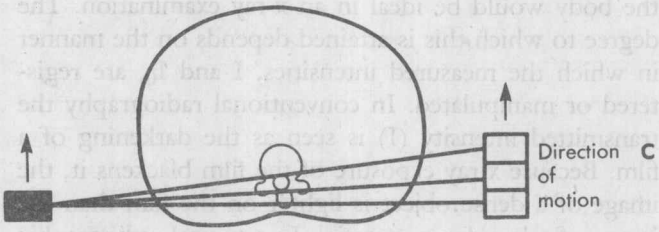

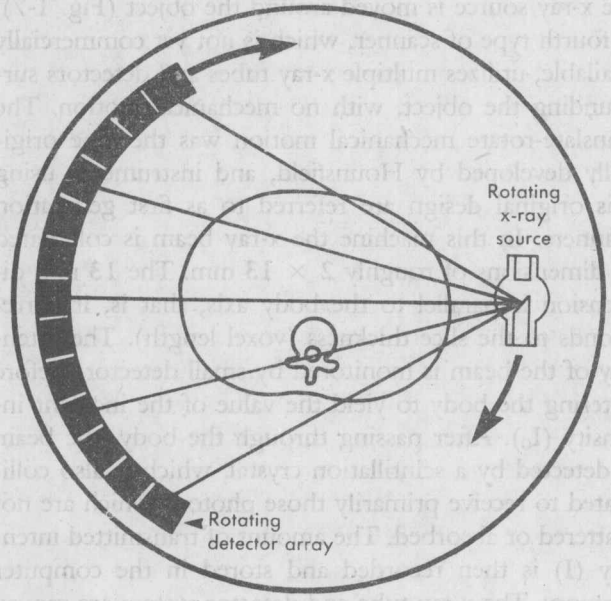

Fig. 1-6. Rotate-only scanner.

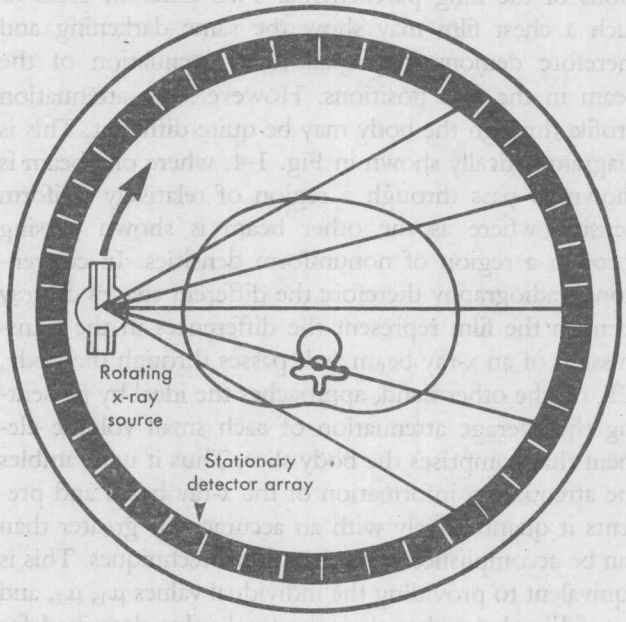

Fig. 1-7. Rotate scanner with stationary detectors.

measurements during the translation. At the end of each translation the x-ray tube and detector system are rotated 1 degree, and the translation is repeated. The translate-rotate process is repeated for 180 translations, which yield 28,800 (160 × 180) measurements. The 160 measurements made during one complete translation are called a *profile,* or *view.*

From a clinical point of view this machine has the major disadvantage of long scanning times. It requires 5 minutes to gather the 28,800 ray sums, which limits its use to body parts such as the head that can be made immobile. The long scanning time provided the impetus to develop other scanning systems.

The first modification was simply to convert the x-ray beam to a fan shape with a diverging angle of between 3 and 10 degrees (Fig. 1-5). Multiple x-ray detectors then were placed adjacent to each other to intercept this beam. Since more x-ray detectors were used, the number of angular rotations could be decreased and an adequate number of views obtained in much shorter intervals. Such second generation scanners were able to obtain a scan in periods as short as 18 seconds. It should be obvious from Fig. 1-5 that each detector obtains a different view during a translation, since the rays from the x-ray tube to the detectors are not parallel.

The next development involved widening the x-ray diverging angle so that it could entirely encompass the object without performing any translatory motion (Fig. 1-6). Thus a rotate-only scanner was developed, and such instruments are referred to as third generation scanners because chronologically they were the third development. In this scanner the gantry rotates continuously. The greatest advantage is that these instruments can produce a scan in approximately 3 to 5 seconds, which is suitable for most body studies. Because these scanners have a spatial resolution that depends primarily on the detector aperture opening and on the number of ray projections gathered in a rotation, it is necessary to have a large number of closely packed detectors intercepting the beam. This eliminates the use of crystal detectors because of their bulk. Consequently gas (e.g., xenon) detector systems were designed, and more recently small solid-state detector systems have been tried.[21] As is usually the case, there are advantages and disadvantages to this system. The gas detectors are less efficient for the detection of x-ray beams and also require high precision in manufacturing. On the other hand, because of their geometry, they tend to eliminate scattered photons and thus decrease image noise.

Removing detector cells from the rotating gantry and mounting them in stationary positions around the patient allowed a further decrease in scanning time to between 1 and 3 seconds (Fig. 1-7). Approximately 600 to 1200 detectors are used in these machines, and generally crystal detectors, such as bismuth germanium oxide or cesium iodide, are used for highly efficient capturing of x-ray photons. The chronological development of these machines yields the name fourth generation scanners. In this scanner the x-ray tube is on continuously during a scan, and each detector receives x-ray beams for a significant portion of the scan cycle.

Although both fourth and third generation scanners have the similarity of rotation, they are very different in principle. In the rotate-only moving detector system each detector has a fixed relationship with the x-ray tube. This fixed relationship allows the detector to be highly collimated, which greatly reduces scattered radiation, and, as discussed later, this reduces image noise. Such an arrangement provides the best situation for low-contrast resolution. In the stationary detector system with a rotating x-ray tube the detectors cannot be

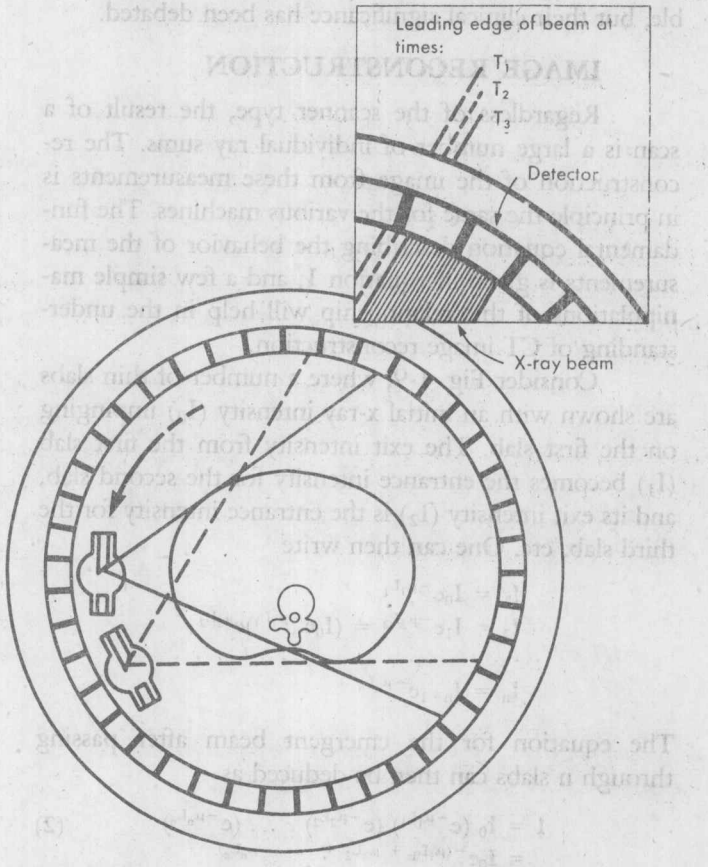

Fig. 1-8. Overlapped measurements. Leading edge of the x-ray beam is shown at three different times (T_1, T_2, and T_3) during a scan. Differencing the detector response for the various contiguous intervals yields equivalent nonoverlapped ray projections.

highly collimated because they would then only contribute data when the x-ray tube was directly opposite. This would severely limit the total number of ray sums to the number of detectors and yield an unacceptably low number of projections. To overcome this problem, the detectors are collimated with wide apertures that permit them to gather radiation over a wide angle (Fig. 1-8). In this manner the x-ray beam overlaps a number of detectors. Over contiguous intervals the amount of detectors intercepting the beam varies, as does the particular grouping of detectors. Mathematically manipulating these overlapped data measurements allows a large number of closely spaced, narrow, equivalent ray sums to be obtained. The result can lead to a very high spatial resolution but also causes an increase in detection of scattered radiation, even though some of this scattering is removed by appropriate patient-to-detector spacing. Concomitantly there is an increase in image noise that diminishes the density-resolution capability of the instrument. These theoretical differences between third and fourth generation scanners are real and demonstrable, but their clinical significance has been debated.

IMAGE RECONSTRUCTION

Regardless of the scanner type, the result of a scan is a large number of individual ray sums. The reconstruction of the image from these measurements is in principle the same for the various machines. The fundamental equation describing the behavior of the measurements is given in equation 1, and a few simple manipulations of this relationship will help in the understanding of CT image reconstruction.

Consider Fig. 1-9, where a number of thin slabs are shown with an initial x-ray intensity (I_0) impinging on the first slab. The exit intensity from the first slab (I_1) becomes the entrance intensity for the second slab, and its exit intensity (I_2) is the entrance intensity for the third slab, etc. One can then write

$$I_1 = I_0 e^{-\mu_1 L_1}$$
$$I_2 = I_1 e^{-\mu_2 L_2} = (I_0 e^{-\mu_1 L_1}) e^{\mu_2 L_2}$$
$$\cdots\cdots\cdots\cdots\cdots\cdots$$
$$I_n = I_{n-1} e^{-\mu_n L_n}$$

The equation for the emergent beam after passing through n slabs can then be deduced as

$$I = I_0 (e^{-\mu_1 L_1})(e^{-\mu_2 L_2}) \cdots (e^{-\mu_n L_n}) \quad (2)$$
$$= I_0 e^{-(\mu_1 L_1 + \mu_2 L_2 + \cdots + \mu_n L_n)}$$

For simplicity the subscript n on I_n has been dropped. Therefore the total attenuation is equivalent to the simple equation

$$I = I_0 e^{-\mu L} \quad (3)$$

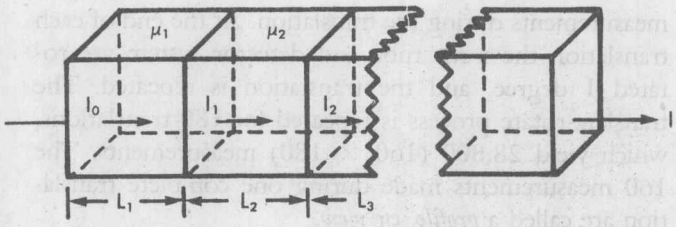

Fig. 1-9. Illustration of equation 2.

where

$$\mu L = \mu_1 L_1 + \mu_2 L_2 + \cdots + \mu_n L_n \quad (4)$$

In the case where $L_1 = L_2 = L_3 = \cdots = L_n$, that is, all the slabs have equal thickness, equation 4 can be written as

$$\mu L = (\mu_1 + \mu_2 + \cdots + \mu_n) L \quad (5)$$

If one now takes the logarithm of both sides of equation 3 and rearranges it, the result is

$$\mu = (\mu_1 + \mu_2 + \cdots + \mu_n) = \frac{1}{L} \ln \frac{I_0}{I} \quad (6)$$

This equation shows that, if the incident intensity I_0, transmitted intensity I, and segment length L are known, the sum of the attenuation coefficients along the path of the x-ray beam can be calculated.

Because there are n unknowns (one for each segment), each value of the attenuation coefficient cannot be determined from a single equation. Algebraic theory requires that there be n independent equations to obtain solutions for the n unknown values of μ. To get n independent equations, a number of views must be taken; it is then possible to gather sufficient data for the multiple equations. A comparison again with conventional radiography shows that, since only one measurement is made in radiography, only the average value of μ or the sum of the μL's can be obtained. Thus the information on the film is less detailed than the information on a CT image.

The reconstruction process

For each ray projection measurement made during a CT scan, one equation 6 is generated, and the complete set of such equations then must be solved to obtain the individual values of μ for each matrix element. Since there are thousands of ray projections obtained for a scan, there are thousands of equations to be solved simultaneously, and the need for high-speed computers is obvious. It must be noted that L is not related to the slice thickness (voxel length) and is chosen

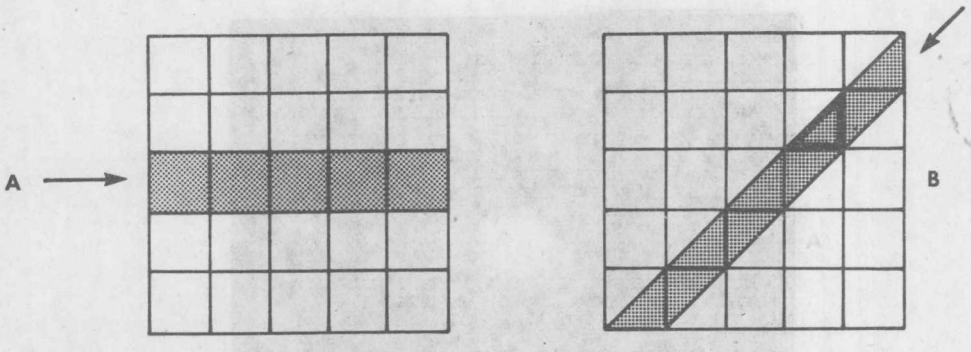

Fig. 1-10. Ray projections. **A,** The projection includes only voxels parallel to the matrix representation, and entire voxels are covered. **B,** The projection is oblique to the matrix. A weighting factor must be included for the back projections to avoid giving these pixels undue influence.

for the reconstruction process by selecting a matrix size. Provided sufficient ray projections have been made, the image can be reconstructed in any matrix size, which is paramount to choosing any value of L. The voxel length is set by the collimation of the scanner when a slice thickness is selected. *A picture element (pixel) therefore represents the attenuation coefficient (μ) of a volume element with length determined by the slice thickness chosen during the data acquisition and cross-sectional area that has a side dimension (L) chosen at the time of reconstruction.*

Many methods have been devised to solve the set of equations generated in a scan; however, most manufacturers today have settled on the *filtered back-projection* method because it allows short computation time with relatively accurate solutions.* It also allows processing of each ray sum immediately after it is obtained while the data acquisition continues for other ray sums. This permits the final image to be available for viewing almost immediately after completion of the scanning process. It is important to understand the basic concepts underlying reconstruction procedures, since their manner of application affects the quality of the final image.

The back-projection method is an attempt to approximate the solution by projection of a uniform value of attenuation over the path of the ray such that the calculated attenuation over the path is proportional to the measured attenuation. These values then are stored in the computer for the matrix elements involved, and the process is repeated for each ray sum of the scan. Each matrix element thus receives a contribution from each ray that passes through it. For those voxels through which the beam passes obliquely, a correction is made to the contribution (Fig. 1-10). The final image so obtained is rather blurred as a result of the assumption that the beam attenuation occurs uniformly over the entire path of the ray. The process is exemplified in Fig. 1-11, which demonstrates the result of applying this procedure to a uniform field with a circular object of high-density imbedded in it. In the example only a few rays are used. Two observations should be made: (1) the procedure generates a starburst pattern, and (2) it tends to approximate the image better as more views are obtained.

No matter how many views are used, however, the blurring effect is never completely eliminated. Thus a second mathematical maneuver called a *convolution operation,* or *filtering process,* is used.[5,13] The purpose of the filtering process is to modify the ray sum data such that the back projections consist of both positive and negative values. In the example of Fig. 1-12 the profile of the back-projected density is modified to look like the one shown in *B* rather than that in *A*. The result is the cancellation of some of the back-projected densities of other ray sums and removal of the unsharpness.

The filtering procedure involves a mathematical operation on the ray sum with a "filter function" or convolution "kernel." The filter function is a complex one that depends on many parameters, including x-ray tube geometry and detectors, and can take on a number of forms depending on the desired result.[3,10] For example, one form of the filter function might enhance edges and thus sharpen the image, whereas another will blur edges for more gradual density changes. The edge-sharpening filter will enhance spatial resolution but simultaneously will decrease density resolution. Thus the choice of filter or kernel affects image quality, and the radiologist should be able to choose the best filter for a particular study. Some manufacturers automatically select the fil-

*References 2, 4, 5, 8, and 9.